Extensive fibrosis in mediastinal seminoma is a diagnostic pitfall in small biopsies: two case reports

Anthony R. Liccardi[1], Kristen Thomas[2], Navneet Narula[2], Lea Azour[3]^, Andre L. Moreira[1,2]^, Fang Zhou[2]^

[1]Center for Biospecimen Research and Development, Office of Science and Research, New York University Grossman School of Medicine, New York, NY, USA; [2]Department of Pathology, New York University Langone Health, New York, NY, USA; [3]Department of Radiology, New York University Langone Health, New York, NY, USA

Correspondence to: Fang Zhou, MD. Assistant Professor of Pathology, Department of Pathology, New York University Langone Health, 560 First Avenue, New York, NY 10016, USA. Email: fang.zhou@nyu.edu.

Background: In mediastinal biopsies that show fibrosis, the differential diagnosis includes fibrosing mediastinitis, immunoglobulin G subclass 4-related disease, Hodgkin lymphoma, as well as reactive fibrotic and inflammatory changes adjacent to other processes including neoplasms.

Cases Description: We report two cases of incidentally detected mediastinal seminoma that contained extensive areas of paucicellular fibrosis, which precluded accurate preoperative biopsy diagnosis. The fibrosis consisted of mildly inflamed, densely scarred tissue with thin dilated vessels, and was present to a significant extent that is suggestive of spontaneous regression. These features are not currently described in the World Health Organization Classification of Thoracic Tumors. In both patients, needle and open biopsies sampled only the fibrotic areas of the tumors, and the final diagnosis was not achieved until surgical excision was performed. After surgery, both patients received chemotherapy, and were alive without evidence of disease at 3.4 years and 1 year post-operatively, respectively. Tumor fibrosis composed approximately 95% and 50% of each patient's tumor, respectively. In one of the patients, correlation of the needle biopsy position with the positron emission tomography (PET) scan revealed that the biopsy needle had sampled a non-metabolically active portion of the tumor.

Conclusions: While pathologic spontaneous regression is well-described in gonadal germ cell tumors, it is not well-reported in extragonadal locations. Prospective knowledge of this diagnostic pitfall and targeting PET-avid regions of the tumor may increase the diagnostic yield and help to avoid non-indicated surgical interventions.

Keywords: Mediastinal; seminoma; regression; case report

Introduction

The mediastinum can be affected by many different types of tumors and inflammatory conditions, with differing therapeutic options. Therefore, the work-up of an anterior/prevascular mediastinal mass includes clinical, laboratory (serum β-human chorionic gonadotropin (β-hCG), alpha fetal protein (AFP), lactate dehydrogenase (LDH), carcinoembryonic antigen (CEA), and autoantibodies against acetylcholine receptors), and imaging studies to hone the differential diagnosis and clarify the extent of disease. Primary mediastinal seminomas, while rare, are the
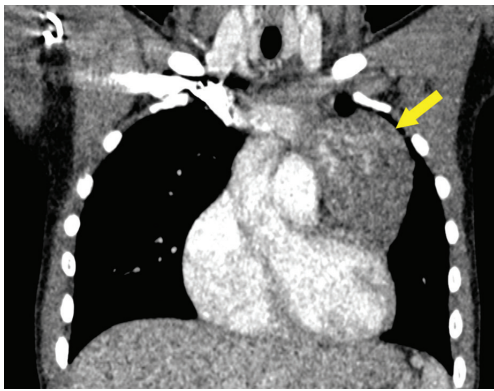
Figure 1 Case 1 imaging. Coronal contrast-enhanced pediatric protocol low dose CT showed a left prevascular mediastinal mass (arrow) that is well-circumscribed, and lobulated, with serpiginous heterogeneous enhancement. CT, computed tomography.

second most common (10–37%) primary germ cell tumor of the mediastinum, behind teratomas. Mediastinal seminoma occurs almost exclusively in young men, more frequently in the second and fourth decades (range, 9 to 79 years old) (1). Most patients are asymptomatic, with incidental discovery of a large mediastinal mass (1). Their serum markers are frequently within normal limits, although mildly elevated β-hCG and LDH levels have been reported. On imaging studies, mediastinal seminoma usually presents as a large and homogeneous mass with mild enhancement on contrast-enhanced computed tomography (CT) (2), which is radiographically nonspecific. Therefore, tissue sampling, most often by core needle or fine needle aspiration biopsy, is necessary for diagnosis. The most commonly recommended management of patients with seminoma is systemic platinum-based chemotherapy, or radiation for localized disease if chemotherapy is contraindicated. Surgery may be considered as salvage therapy, but is not recommended as the primary modality of therapy, unless the tumor is very small and localized (3-6).

Here we report two cases in which preoperative clinical evaluation and biopsies failed to render a specific diagnosis of primary mediastinal seminoma, leading to surgical excision. Pathologic examination of both resected tumors revealed extensive areas of fibrosis suggestive of spontaneous tumor regression. Tumor regression is not well-defined, and there is no standard for grading regression. Some have proposed scoring tumor regression by comparing the volume of viable tumor cells to the volume of fibrosis (7). Fibrous septa/stroma is mentioned in the morphologic

description of primary mediastinal seminoma in the World Health Organization (WHO) Classification of Thoracic Tumors (1), and it is seen in many slow-growing tumors. However, extensive fibrosis to the degree seen in our cases is not described by the WHO book, and is not well-described in the existing literature (1). It is important to raise awareness of this diagnostic pitfall in mediastinal biopsies (8,9). We present the following cases in accordance with the CARE reporting checklist (available at https://med.amegroups.com/article/view/10.21037/med-22-15/rc).

Case presentation

Case 1

A 14-year-old male patient presented for workup of shoulder pain and concern for shoulder asymmetry following a sports injury. He denied chest pain and shortness of breath. He had a history of growth hormone deficiency, and was on daily growth hormone replacement therapy. Physical exam was unremarkable, including lack of significant shoulder asymmetry. Single view anteroposterior (AP) chest radiograph incidentally showed a left sided mediastinal contour abnormality concerning for a mediastinal mass. Chest CT with contrast showed a large lobulated, heterogeneous, and vascular left prevascular mediastinal mass isodense to surrounding soft tissue, with internal areas of enhancement (*Figure 1*). Serum AFP and β-hCG were within normal limits. Scrotal Doppler ultrasound study showed no testicular mass. Abdominopelvic magnetic resonance imaging (MRI) and brain MRI were normal.

CT-guided biopsy yielded scant fragments of fibroconnective tissue with variable collagenization and myxoid change (*Figure 2*) associated with irregular and thin ectatic vessels. The stroma was variably cellular and contained reactive myofibroblasts, which were positive on immunohistochemical stains (IHC) for smooth muscle actin (SMA), had mild non-specific reactivity with pancytokeratin AE1/AE3, and were negative for S100 protein. Given the nonspecific findings, additional tissue sampling was performed.

An open biopsy (Chamberlain procedure) showed extensive fibrosclerosis, lymphoplasmacytic inflammatory infiltration, and thin dilated vessels (*Figure 3*). IHC for spalt like transcription factor 4 (SALL4), a pan-germ cell marker, was negative. Cluster of differentiation 34 (CD34), SMA, and desmin highlighted an abundant vascular component. ALK (D5F3), β-catenin, calponin, caldesmon, epithelial
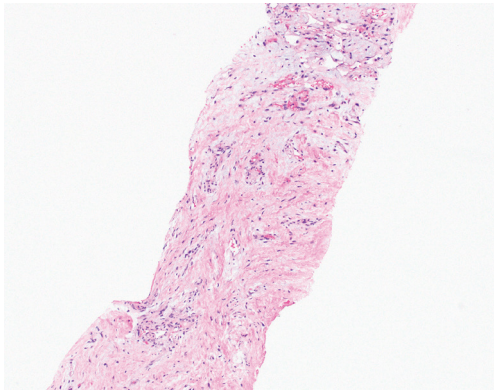
Figure 2 Case 1 first biopsy. CT-guided biopsy was nonspecific. There was scant fibroconnective tissue with variable collagenization, myxoid change, and myofibroblasts (H&E stain; original magnification: 100×). Additional tissue sampling was recommended. CT, computed tomography; H&E, hematoxylin and eosin.
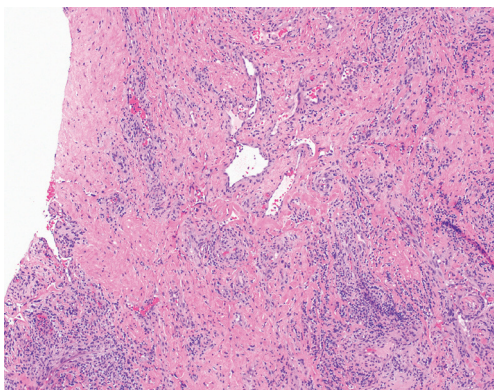

Figure 3 Case 1 second biopsy. Open biopsy showed extensive fibrosclerosis, lymphoplasmacytic infiltration, and thin dilated vessels (H&E stain; original magnification: 100×). H&E, hematoxylin and eosin.

membrane antigen (EMA), and S100 protein were negative. Chromogenic in-situ hybridization for EBV [Epstein Barr virus encoded RNA (EBER)] was also negative. The diagnosis was "vascular fibroblastic/myofibroblastic proliferation consistent with a reactive process".

Complete surgical resection of this lesion by left posterolateral thoracotomy was performed. Gross exam showed a 7.0 cm × 6.9 cm × 4.3 cm irregular circumscribed red-pink firm mass with mottled fibrotic cut surfaces (*Figure 4A*). Microscopic evaluation revealed that the vast majority of the mass consisted of mildly inflamed vascular

sclerotic tissue morphologically similar to the previous two biopsies. Only approximately 5% of the total mass contained sheets of medium-sized malignant cells with relatively uniform, large central nuclei with prominent nucleoli, and amphiphilic to clear cytoplasm. The malignant cells were located mostly along the periphery of the mass and involved adjacent thymic parenchyma (*Figure 4B,4C*). IHC showed the tumor cells were diffusely and strongly positive for octamer-binding transcription factor-4 (OCT-4), cluster of differentiation 117 (CD117), placental-like alkaline phosphatase (PLAP) (*Figure 4D-4F*), and podoplanin (D2-40), while negative for AFP and S100 protein. The morphologic and IHC findings were diagnostic of seminoma. Resection margins were negative. One month post-resection, the patient started 4 cycles of chemotherapy (bleomycin, etoposide and cisplatin), which were completed in 80 days. There was no evidence of disease in 3.4 years of post-operative follow-up with serum and imaging studies. *Table 1* summarizes the timeline of events for this patient.

Case 2

A 66-year-old male with history of atrial flutter, Factor V Leiden, and coronavirus disease of 19 (COVID-19) infection (7 months prior) sought emergency care after an episode of syncope. Physical exam was unremarkable. CT pulmonary angiogram demonstrated pulmonary embolism, as well as an incidental large prevascular mediastinal mass with small peripheral calcifications (*Figure 5*). The mass was fluorodeoxyglucose (FDG)-avid on positron emission tomography (PET)-CT, with standardized uptake value (SUV) of 6.3, which was suspicious for malignancy. Upon retrospective review, approximately 50% of the mass was FDG-avid, while the remainder was not FDG-avid. The PET scan showed no evidence of metastatic disease, and no other mass, including in the head, retroperitoneum, coccyx, or scrotum. Seven and a half weeks before biopsy and 9 weeks before surgery, serum LDH was mildly elevated to 317 U/L (reference range, 125–220 U/L); 3.5 weeks before biopsy and 5 weeks before surgery, repeat serum LDH was within normal range. Serum β-hCG, AFP, and CEA levels were within normal limits.

CT-guided biopsy was performed, with the needle (*Figure 6A*) passing through a portion of the mass that was not FDG-avid (*Figure 6B*). The biopsy demonstrated hypocellular dense fibrous tissue (*Figure 6C*). Congo red stain for amyloid was negative. IHC for signal transducer
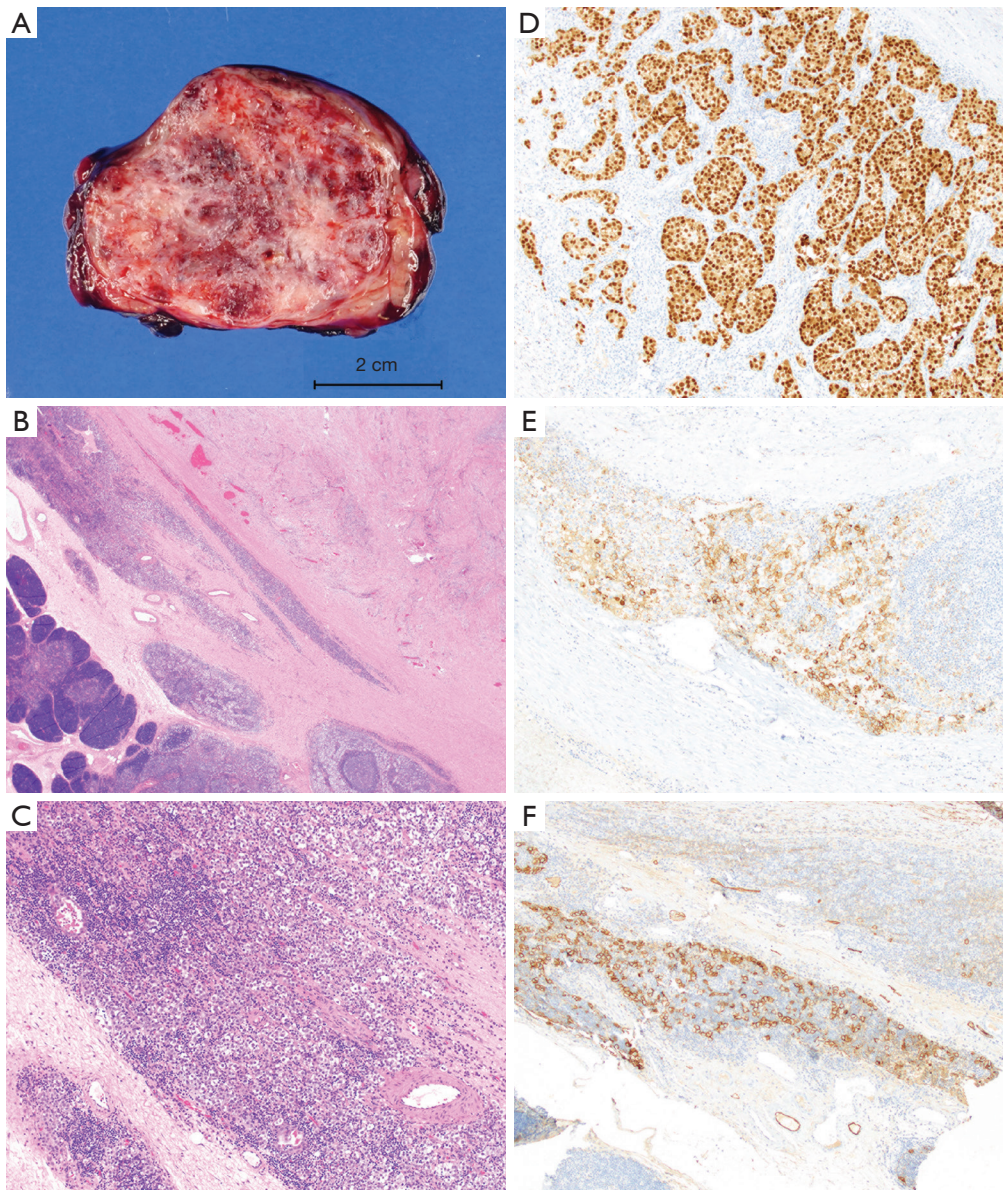
Figure 4 Case 1 resection. Gross examination of the resection specimen showed a 115.6 g, 7.0 cm × 6.9 cm × 4.3 cm irregular well-circumscribed, red-pink firm mass with mottled fibrotic cut surfaces (A). Only approximately 5% of the mass showed tumor cells, mostly along the periphery and involving adjacent thymic parenchyma (B, middle and bottom; H&E stain; original magnification: 20×). The remainder of the mass consisted of inflamed vascular sclerotic tissue suggestive of regression (B, upper right). The tumor component consisted of sheets of medium-sized tumor cells with relatively uniform, large central nuclei with prominent nucleoli, and amphiphilic to clear cytoplasm (C; H&E stain; original magnification: 100×). The tumor cells were positive for immunostains OCT-4, PLAP, and D2-40, consistent with seminoma (D, E, F, respectively; immunohistochemical stains; original magnification: 100×). H&E, hematoxylin and eosin; OCT-4, octamer-binding transcription factor-4; PLAP, placental-like alkaline phosphatase; D2-40, podoplanin.

Table 1 Timeline of events for case 1

Day	Event
−181 (6 months before mass was discovered)	Brain MRI was normal
0	A 14-year-old boy with history of growth hormone deficiency, on daily growth hormone replacement therapy, presented for workup of shoulder pain and concern for shoulder asymmetry after a sports injury. No shoulder abnormality was diagnosed
0	Chest radiograph incidentally discovered a large chest mass
3	Chest CT with contrast showed a large lobulated, heterogeneous, vascular left prevascular mediastinal mass. No lymphadenopathy
6	Serum AFP and β-hCG were normal
8	CT-guided biopsy of the mediastinal mass showed scant fibroconnective tissue with myxoid change, variable cellularity, and irregular thin ectatic vessels. Additional sampling was recommended
13	Open biopsy (Chamberlain procedure) showed extensive fibrosclerosis, lymphoplasmacytic inflammation, and dilated vessels, consistent with a reactive process
29	Complete surgical resection showed a 7-cm seminoma with approximately 95% fibrosis that contained lymphoplasmacytic infiltrates and irregular thin ectatic vessels. The 5% of the mass that contained viable tumor cells was located along the periphery of the tumor, involving adjacent thymic parenchyma. Resection margins were negative
37	US of scrotum was negative
40	MRI of abdomen/pelvis was negative
60 to 140	4 cycles of chemotherapy were completed (bleomycin, etoposide, cisplatin)
1,261 (3.4 years after resection)	No evidence of disease

MRI, magnetic resonance imaging; CT, computed tomography; AFP, alpha fetoprotein; hCG, human chorionic gonadotropin; US, ultrasound.
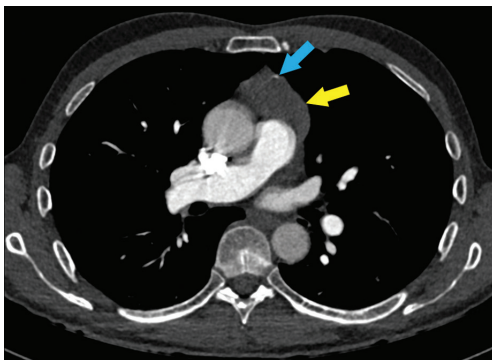

Figure 5 Case 2 imaging. Axial CT angiogram of the chest showed a prevascular mediastinal mass (yellow arrow) with small peripheral calcifications (blue arrow). CT, computed tomography.

and activator of transcription 6 (STAT6), S100 protein, and β-catenin were negative. Flow cytometry analysis was negative for non-Hodgkin lymphoma.

The patient underwent a robotic thymectomy. Gross

examination demonstrated a 7 cm × 6 cm × 1.5 cm lobulated tan-white firm tumor with focal hemorrhage (*Figure 7A*). Microscopic exam showed approximately 50% of the tumor consisted of a well-defined region of hypocellular dense fibrous tissue that was similar to what was seen in the preoperative biopsy. The resection additionally showed areas within the fibrosis that contained irregular thin ectatic vessels similar to the first case (*Figure 7B*). The tumor consisted of sheets and nests of medium sized cells separated by fibrous septa. Similar to the first case, the tumor cells also had amphiphilic to clear cytoplasm with relatively uniform, large central nuclei and prominent nucleoli. A lymphoplasmacytic infiltrate was seen in the fibrous septa (*Figure 7C*). IHCs showed the tumor cells were positive for OCT-4 (*Figure 7D*), CD117 (*Figure 7E*), SALL4 (*Figure 7F*), pancytokeratin CAM 5.2 (dot-like cytoplasmic pattern), and D2-40, while negative for Glypican-3 and cluster of differentiation 30 (CD30), which confirmed the diagnosis of seminoma. The resection margin was focally positive. No lymph node metastasis was present. Three and a half
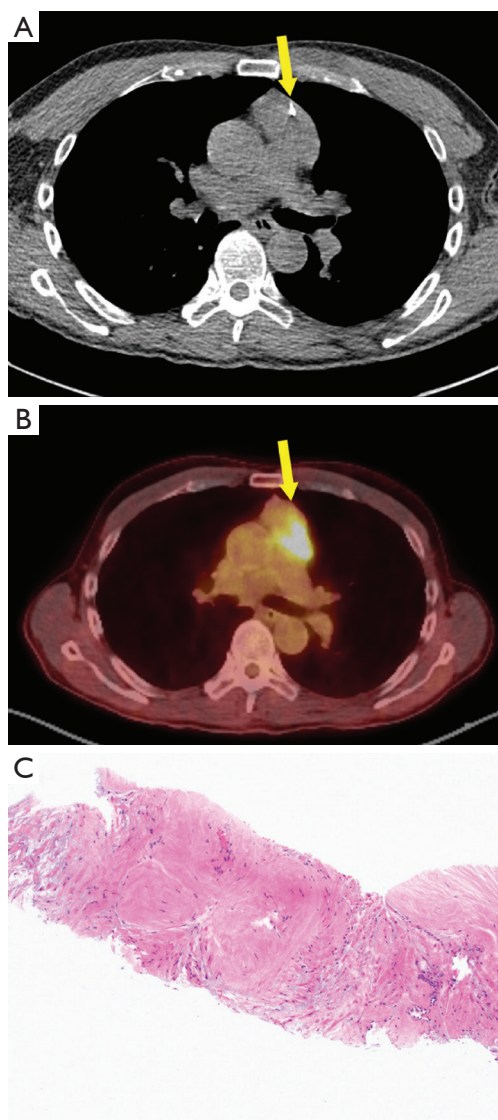
Figure 6 Case 2 biopsy. During CT-guided biopsy, the needle (A, arrow) entered a non-FDG-avid portion of the mass (B; PET scan; arrow corresponds to biopsied area shown in A). The biopsy demonstrated hypocellular dense fibrous tissue (C; H&E stain; original magnification: 100×) that was negative for Congo red, STAT6, S100 protein, and β-catenin. CT, computed tomography; FDG, fluorodeoxyglucose; PET, positron emission tomography; H&E, hematoxylin and eosin.

months post-resection, the patient underwent 4 cycles of chemotherapy (etoposide and cisplatin), which were completed in 67 days. There was no evidence of disease in 1 year of post-operative follow up with serum and imaging studies. *Table 2* summarizes the timeline of events for this

patient.

All procedures performed in this study were in accordance with the ethical standards of the institutional and/or national research committee(s) and with the Helsinki Declaration (as revised in 2013). The study was approved by the institutional review board of New York University (No. S21-01220), and individual consent for this retrospective analysis was waived.

Discussion

Summary & literature review

We have provided what is to date the most detailed clinicopathologic description of two cases of primary mediastinal seminoma with tumor regression. The regressed areas were sampled on biopsy and hindered accurate preoperative diagnosis. Spontaneous tumor regression is a rare phenomenon, and its real incidence is difficult to estimate (10). There is no standard for grading regression. Some have proposed scoring tumor regression according to the volume of radiation-induced or idiopathic (in our cases) fibrosis (7). The underlying mechanisms are unknown. One theory is that it is mediated by immune system activation (11), and some hypothesize it may be akin to a wound-healing process (12). It is well-described in gonadal seminomas, and is recognized in the WHO Classification of Tumors of the Urinary System and Male Genital Organs (13). For mediastinal germ cell tumors, although fibrous septa/stroma is mentioned in the WHO Classification of Thoracic Tumors (1), this type of limited fibrosis is seen in many slow-growing tumors. Extensive fibrosis to the degree consistent with tumor regression, as seen in our cases, is not described by the WHO, and is not well-described in the existing literature (1). It is important to raise awareness of this diagnostic pitfall in mediastinal biopsies (8,9).

In the testis, germ cell tumor regression usually manifests histologically as a well-defined to irregular nodular focus/foci of scar or fibrosis with various combinations of fibrosis, neovasculature, mixed chronic inflammation, calcification, and/or giant cell reaction (13-16). Both of our cases of mediastinal seminoma demonstrated histologic findings that correspond to the features of regression described in gonadal germ cell tumors. They both contained extensive areas of well-defined fibrosis with inflammation and irregular thin-walled ectatic vessels (consistent with neovasculature). In addition, there was transient elevation of serum LDH in patient #2, followed by spontaneous
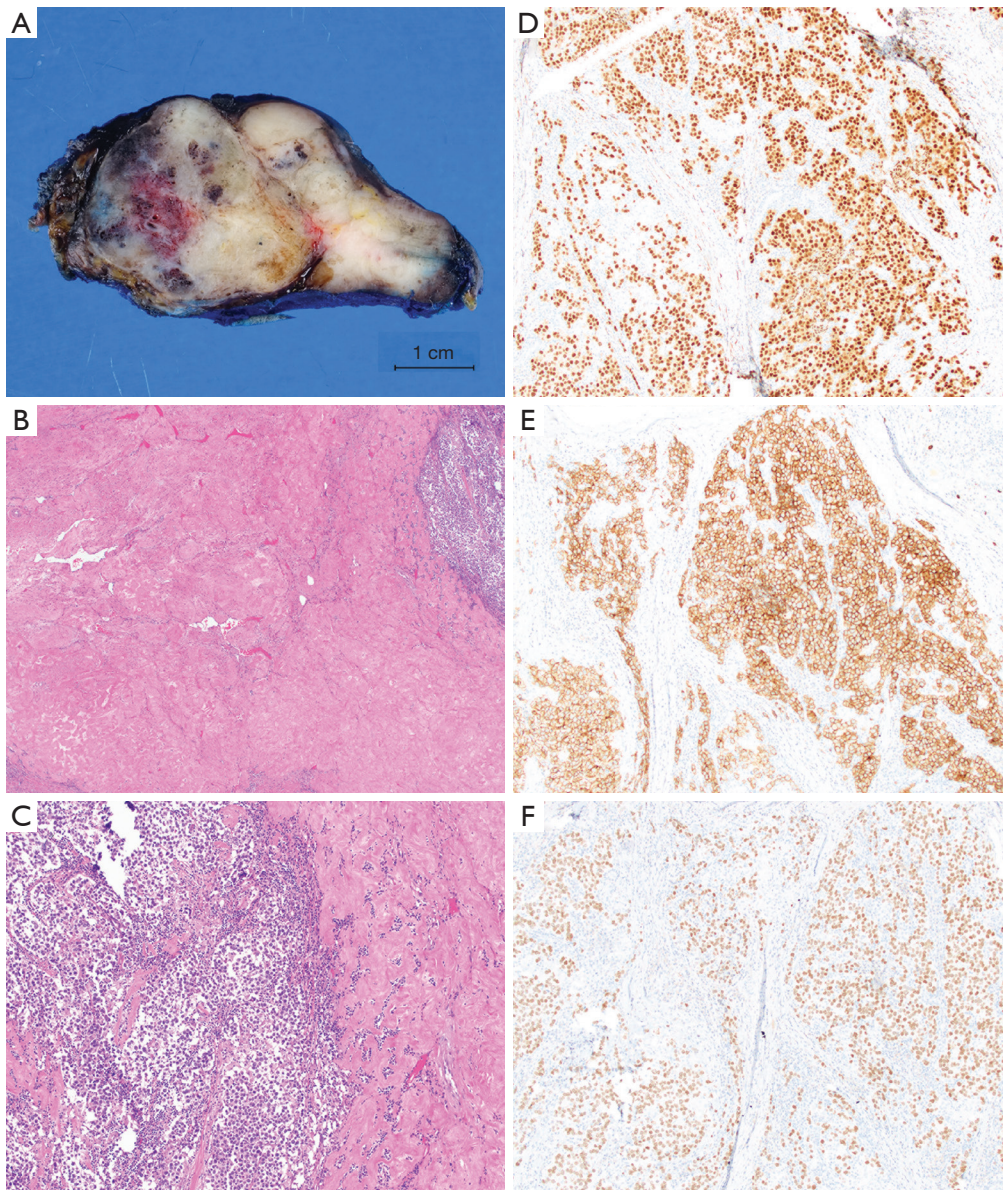
Figure 7 Case 2 resection. Gross examination of the resection specimen showed a 7.0 cm × 6.0 cm × 1.5 cm tan-white lobulated firm tumor with focal hemorrhage on cut sections (A). Approximately 50% of the tumor showed dense hypocellular fibrotic tissue with irregular thin ectatic vessels, suggestive of regression (B, left; H&E stain; original magnification: 40×). The tumor consisted of sheets and nests of medium sized tumor cells separated by fibrous septa. The tumor cells had amphiphilic to clear cytoplasm with relatively uniform, large central nuclei and prominent nucleoli. A lymphoplasmacytic infiltrate was seen in the fibrous septa (C; H&E stain; original magnification: 100×). The tumor cells were positive for immunostains OCT-4, CD117, SALL4 (D, E, F, respectively; immunohistochemical stains; original magnification: 100×), keratin CAM 5.2 (dot-like cytoplasmic pattern), and D2-40, while negative for Glypican-3 and CD30, consistent with seminoma. H&E, hematoxylin and eosin; OCT-4, octamer-binding transcription factor-4; CD117, cluster of differentiation 117; SALL4, spalt like transcription factor 4; D2-40, podoplanin; CD30, cluster of differentiation 30.

Table 2 Timeline of events for case 2

Day	Event
0	A 66-year-old man with history of atrial flutter, Factor V Leiden, and COVID-19 infection (seven months prior) sought emergency care after an episode of syncope
0	CT angiogram showed pulmonary emboli, and incidentally discovered a prevascular mediastinal mass
1	Serum β-hCG, AFP, and CEA levels were normal
22	Serum LDH was elevated to 317 U/L (reference range, 125–220 U/L)
49	Serum LDH decreased to normal
50	PET/CT scan showed the mass had an SUV of 6.3 which was suspicious for malignancy. There was no evidence of metastatic disease or mass elsewhere, including the head, retroperitoneum, coccyx, or scrotum
	In hindsight, approximately 50% of the mediastinal mass showed lack of FDG avidity, corresponding to 50% of the tumor being fibrotic on pathologic examination of the resection specimen
73	CT-guided biopsy showed hypocellular dense fibrous tissue.
85	Surgical resection showed a 7-cm seminoma with approximately 50% fibrosis corresponding to the non-FDG avid portion of tumor on PET scan. Lymphoplasmacytic infiltrates and irregular thin ectatic vessels were present in the fibrosis. Focally positive resection margin. Benign lymph nodes
189 to 256	4 cycles of chemotherapy were completed (etoposide, cisplatin)
455 (1 year after resection)	No evidence of disease

COVID-19, coronavirus disease of 19; CT, computed tomography; hCG, human chorionic gonadotropin; AFP, alpha fetoprotein; CEA, carcinoembryonic antigen; LDH, lactate dehydrogenase; PET, positron emission tomography; SUV, standard uptake value; FDG, fluorodeoxyglucose.

normalization; and upon retrospective review of the PET-CT scan and biopsy needle placement, the fibrotic region corresponded to a non FDG-avid region of the tumor. It is based on these facts that we propose the extensive fibrosis seen in our cases is consistent with regression (7).

In the existing English language literature, only two cases of mediastinal germ cell tumor with spontaneous regression have been reported (*Table 3*). In both cases, serum β-hCG was initially elevated, followed by normalization before any therapy was initiated. CT scans in both cases showed concomitant tumor size decrease as the serum hCG levels decreased. Histologic exam of one resected case showed combined teratoma and seminoma with evidence of regression in the form of fibrous granulation tissue (8). The other case was diagnosed on open biopsy, followed by chemotherapy and resection; histologic features of regression were not described in the paper (9).

Clinical relevance and differential diagnosis

Clinically, the differential diagnosis of an anterior/prevascular mediastinal mass includes (I) benign entities such as enlarged or ectopic thyroid tissue, thymic hyperplasia, and ectopic parathyroid tissue; (II) primary neoplastic diseases including thymic epithelial neoplasms, thymic neuroendocrine neoplasms, lymphoma, and extragonadal germ cell tumor; (III) metastatic disease; as well as (IV) inflammatory diseases, such as infection, lipid storage disease, sarcoidosis, fibrosing mediastinitis, immunoglobulin G subclass 4-related disease (IgG4-RD), histiocytosis X, and Castleman disease (17,18). Biopsy of the lesion is preferred for diagnosis, and contributes to the decision of whether to pursue surgical resection, radiation, or systemic therapy. The sensitivity and specificity of biopsies, including fine needle aspiration, for the diagnosis of mediastinal lesions is very good, although cystic and inflammatory conditions have lower sensitivity (19).

The presence of fibrous tissue in a mediastinal biopsy raises the possibility of the following entities in the pathologic differential diagnosis: fibrosing mediastinitis; IgG4-RD; Hodgkin lymphoma; as well as reactive fibrotic and inflammatory changes within or adjacent to other processes.

Fibrosing mediastinitis, or "sclerosing mediastinitis", is a rare cause of mediastinal masses (20), and is regarded as an abnormal wound-healing response to triggers including

Table 3 Literature review of spontaneous regression in mediastinal germ cell tumors

Paper	Demographics and presentation	Preoperative serum tumor markers	Radiology	Pathology	Chemotherapy	Follow-up after surgery
Hachiya *et al.* 1998, (8)	A 22-year-old man Routine chest radiograph 4-month history of anterior chest pain	Serum hCG was 20 mIU/mL (reference range <1.0 mIU/mL), followed by normalization after needle aspiration biopsy	Postcontrast CT showed the mass decreased in size (unspecified) after needle aspiration biopsy, as serum hCG normalized. A large, low-density area developed	Needle aspiration biopsy was nondiagnostic. Surgical resection showed combined teratoma and seminoma, invading right upper and middle lung lobes, part of pericardium, bilateral brachiocephalic veins, and superior vena cava. No metastasis. Complete resection was achieved. "Most" of the tumor showed regression (fibrous granulation tissue) and large foci of necrosis. Thymic tissue was seen in the mass	Post-surgery: cisplatin, peplomycin, vinblastine	Alive without evidence of recurrence in more than 10 years
Yu *et al.* 2017, (9)	A 37-year-old man Routine chest radiograph Anterior chest discomfort when bending forward	β-hCG 5.9 mIU/mL (reference range <1.0 mIU/mL), followed by spontaneous normalization to 0.9 mIU/mL	CT showed size initially increased from 75 to 83 mm, then decreased to 65 mm as the β-hCG normalized	VATS biopsy showed seminoma. Histopathologic features of regression were not described in the paper. Tumor was fully resected after chemotherapy	Pre-surgery: bleomycin, etoposide, cisplatin	Alive without evidence of recurrence in 2 years
Current paper	A 14-year-old boy Chest radiograph in workup of shoulder pain following a sport injury	β-hCG and AFP within normal limits	CT with contrast showed a heterogeneous mass with internal areas of enhancement	CT-guided and open biopsies were nondiagnostic, showing inflamed sclerotic tissue with irregular thin ectatic vessels. Surgical resection showed seminoma involving thymus. 95% of the tumor showed inflamed vascular sclerotic tissue suggestive of regression. Margins negative	Post-surgery: bleomycin, etoposide, cisplatin (4 cycles)	Alive without evidence of recurrence in 3.4 years
Current paper	A 66-year-old man Chest CT-angiogram in workup of syncope	LDH was elevated to 317 U/L (reference range, 125–220 U/L), followed by spontaneous normalization. β-hCG, AFP, CEA within normal limits	CT pulmonary angiogram showed a mass with small peripheral calcifications. PET scan showed approximately 50% was FDG-avid (SUV 6.3) while the remainder of the tumor was not FDG-avid	CT-guided biopsy of non-FDG-avid region was nondiagnostic, showing dense fibrotic tissue. Surgical resection showed seminoma with 50% hypocellular dense fibrosis with irregular thin ectatic vessels suggestive of regression. Focal positive margin. No nodal metastasis	Post-surgery: cisplatin and etoposide (4 cycles)	Alive without evidence of recurrence in 1 year

hCG, human chorionic gonadotropin; CT, computed tomography; VATS, video-assisted thoracoscopic surgery; AFP, alpha fetoprotein; LDH, lactate dehydrogenase; CEA, carcinoembryonic antigen; PET, positron emission tomography; FDG, fluorodeoxyglucose; SUV, standard uptake value.

histoplasmosis (in which case granulomas may be found), other fungal infections, tuberculosis, autoimmune diseases, and radiation. Radiographically, it often presents as an infiltrative process (21). In most cases, a cause cannot be found; in such idiopathic cases, some presume there may be an undiagnosed underlying infection, autoimmune disease, or IgG4-RD. Histologically, fibrosing mediastinitis can show a range of fibrotic and mixed chronic inflammatory changes that resemble the stages of wound healing (22,23). The fibrosis can consist of fibromyxoid tissue with numerous spindle cells and thin-walled vessels (similar to case 1); or it can consist of thick glassy bands of haphazardly arranged collagen with only focal spindle cells; or it can contain dense hypocellular collagen and occasional dystrophic calcification (similar to case 2). Some have postulated that tumor regression may also be a sort of wound-healing process (12). Unless tumor cells are sampled in the biopsy, it is not possible to separate fibrosing mediastinitis from tumor regression histologically.

IgG4-RD is an autoimmune systemic fibroinflammatory disease characterized by storiform fibrosis with lymphoplasmacytic infiltration, phlebitis, and increased numbers of IgG4-positive plasma cells. Elevated serum levels of IgG4 may or may not be present (24,25). IgG4-RD has been described in the mediastinum (26,27). In our cases, there were no elevated numbers of plasma cells in the biopsies to suggest this diagnosis.

Nodular sclerosis (classical) Hodgkin lymphoma is the most common type of lymphoma to affect the mediastinum. Histologically, the tumor is characterized by nodules of polymorphous inflammatory cells surrounded by broad fibrous bands. Reed-Sternberg cells are required for histopathological diagnosis. Similar to seminoma, poorly-formed granulomata can be seen in association with classical Hodgkin lymphoma. The presence of extensive sclerosis in biopsy specimens can also hinder the diagnosis of this entity.

Conclusions

In cases like ours where fibrosis comprises the majority of the lesion, biopsy diagnosis can be very challenging. The biopsy sample may not reveal the true nature of the lesion that may be present nearby, even with the use of ancillary studies such as immunohistochemistry. Pathologists should always question whether the observed findings account for the entire lesion, or represent reactive or fibrotic changes associated with a different underlying lesion. Here we also

postulate that primary mediastinal seminomas can contain extensive areas of fibrosis (beyond just fibrous septa/stroma) consistent with tumor regression. Prospective knowledge of this diagnostic pitfall and attempts to target biopsies toward FDG-avid portions of a mediastinal mass may increase diagnostic yield and accuracy, thereby helping to prevent non-indicated surgical interventions.

Acknowledgments

Footnote

References

1. WHO Classification of Tumours Editorial Board. Thoracic tumours. 5 edition. Lyon (France): International

Agency for Research on Cancer, 2021.

2. Azour L, Moreira AL, Washer SL, et al. Radiologic and pathologic correlation of anterior mediastinal lesions. Mediastinum 2020;4:5.

3. Rosti G, Secondino S, Necchi A, et al. Primary mediastinal germ cell tumors. Semin Oncol 2019;46:107-11.

4. Dechaphunkul A, Sakdejayont S, Sathitruangsak C, et al. Clinical Characteristics and Treatment Outcomes of Patients with Primary Mediastinal Germ Cell Tumors: 10-Years' Experience at a Single Institution with a Bleomycin-Containing Regimen. Oncol Res Treat 2016;39:688-94.

5. Beyer J, Albers P, Altena R, et al. Maintaining success, reducing treatment burden, focusing on survivorship: highlights from the third European consensus conference on diagnosis and treatment of germ-cell cancer. Ann Oncol 2013;24:878-88.

6. Giunta EF, Ottaviano M, Mosca A, et al. Standard versus high-dose chemotherapy in mediastinal germ cell tumors: a narrative review. Mediastinum 2022;6:6.

7. Min BS, Kim NK, Pyo JY, et al. Clinical impact of tumor regression grade after preoperative chemoradiation for locally advanced rectal cancer: subset analyses in lymph node negative patients. J Korean Soc Coloproctol 2011;27:31-40.

8. Hachiya T, Koizumi T, Hayasaka M, et al. Spontaneous regression of primary mediastinal germ cell tumor. Jpn J Clin Oncol 1998;28:281-3.

9. Yu Z, Kimura D, Tsushima T, et al. Spontaneous regression of anterior mediastinal seminoma with normalization of β-human chorionic gonadotropin levels. Int J Surg Case Rep 2017;39:199-202.

10. Cole WH. Efforts to explain spontaneous regression of cancer. J Surg Oncol 1981;17:201-9.

11. Salman T. Spontaneous tumor regression. Journal of Oncological Science 2016;2:1-4.

12. Roden AC, Moreira AL. editors. Mediastinal Lesions Diagnostic Pearls for Interpretation of Small Biopsies and Cytology. 1st edition. Springer, 2017.

13. Moch H, Humphrey PA, Ulbright TM. editors. WHO classification of tumours of the urinary system and male genital organs. 4 edition. Lyon (France): International Agency for Research on Cancer, 2016.

14. Balzer BL, Ulbright TM. Spontaneous regression of testicular germ cell tumors: an analysis of 42 cases. Am J Surg Pathol 2006;30:858-65.

15. Duarte C, Gilbert DM, Sheridan AD, et al. Spontaneous regression of an extragonadal seminomatous germ cell tumor. Cancer Treat Res Commun 2021;28:100383.

16. Iannantuono GM, Strigari L, Roselli M, et al. A scoping review on the "burned out" or "burnt out" testicular cancer: When a rare phenomenon deserves more attention. Crit Rev Oncol Hematol 2021;165:103452.

17. Almeida PT, Heller D. Anterior Mediastinal Mass. StatPearls. Treasure Island (FL), 2021.

18. Juanpere S, Cañete N, Ortuño P, et al. A diagnostic approach to the mediastinal masses. Insights Imaging 2013;4:29-52.

19. Marcus A, Narula N, Kamel MK, et al. Sensitivity and specificity of fine needle aspiration for the diagnosis of mediastinal lesions. Ann Diagn Pathol 2019;39:69-73.

20. Rossi SE, McAdams HP, Rosado-de-Christenson ML, et al. Fibrosing mediastinitis. Radiographics 2001;21:737-57.

21. Garrana SH, Buckley JR, Rosado-de-Christenson ML, et al. Multimodality Imaging of Focal and Diffuse Fibrosing Mediastinitis. Radiographics 2019;39:651-67.

22. Flieder DB, Suster S, Moran CA. Idiopathic fibroinflammatory (fibrosing/sclerosing) lesions of the mediastinum: a study of 30 cases with emphasis on morphologic heterogeneity. Mod Pathol 1999;12:257-64.

23. Ko SF, Ng SH, Hsiao CC, et al. Juvenile fibromatosis of the posterior mediastinum with intraspinal extension. AJNR Am J Neuroradiol 1996;17:522-4.

24. Deshpande V, Zen Y, Chan JK, et al. Consensus statement on the pathology of IgG4-related disease. Mod Pathol 2012;25:1181-92.

25. Al-Khalili OM, Erickson AR. IgG-4 Related Disease: An Introduction. Mo Med 2018;115:253-6.

26. Hino H, Tanaka N, Matsui H, et al. Isolated middle mediastinal mass associated with immunoglobulin G4-related disease. Surg Case Rep 2021;7:69.

27. Matsui H, Utsumi T, Maru N, et al. A case of IgG4-related anterior mediastinal sclerosing disease coexisting with autoimmune pancreatitis. Surg Case Rep 2020;6:180.